Organic Process Research & Development **2008,** *12,* 860–868

Comparison of the Crystal Chemistry, the Process Conditions for Crystallization and the Relative Structural Stability of Two Polymorphic Forms of N^G-monomethyl-L-arginine Hydrochloride

Spoorthi Dharmayat,[†] Robert B. Hammond,[†,*] Colin Kilner,[‡] Xiaojun Lai,[†] Rex A. Palmer,[§] Brian S. Potter,[§] Christopher M. Rayner,[‡] and Kevin J. Roberts[†]

Institute of Particle Science and Engineering, School of Process, Environmental and Materials Engineering, University of Leeds, Leeds LS2 9JT, U.K., School of Chemistry, University of Leeds, Leeds LS2 9JT, U.K., and School of Crystallography, Birkbeck College, Malet Street, London WC1E 7HX, U.K.

Abstract:

Crystal structures of two conformational polymorphs (Form A and Form D) of N^G-monomethyl-L-arginine hydrochloride, a drug developed to treat septic shock, are presented. Form A is orthorhombic in a tetra-molecular unit cell and Form D is monoclinic in a bimolecular unit cell (space groups $P2_12_12_1$ and $P2_1$, respectively). The two forms display differences in the conformation of the terminal *N*-methyl group, which is *cis* in Form D and *trans* in Form A. Structural energy calculations demonstrate that Form D has a lower lattice energy compared to Form A (−134.7 and −128.8 kcal/mol, respectively). This is supported by solution stability studies where the potential for solution-mediated phase transformation was investigated and Form D is found to be the more stable polymorphic structure at room temperature. The melting behavior of forms A and D indicates a monotropic phase transformation relationship between the two polymorphic forms albeit their melting points (215.7 and 203.7 °C for forms A and D, respectively) would be more consistent with enantiotropic behavior. Solution-mediated phase transformation is thought to be the likely mechanism for monotropic phase interconversion between the two polymorphs. Graph set analysis of the hydrogen bond patterns for both forms reveals the respective first-order graph sets to consist solely of chain motifs involving only the cation moieties. The overall hydrogen bond patterns for both forms were also found to exhibit characteristic packing motifs around the chloride counterion associated with it acting as a hydrogen bond acceptor, bonding to donor groups from three different molecular cations. In this respect, Form A hydrogen bonds with two donor groups towards the carboxylic end and one towards the *N*-methyl end of the molecular cation and Form D hydrogen bonds with two donor groups towards the *N*-methyl end and one towards the carboxylic end. With the presence of a high number of hydrogen bond donors and acceptors, the potential for the formation of other packing motifs and associated polymorphic forms is reviewed.

Introduction

Nitric oxide (NO) is a universal messenger-molecule that is formed from the amino acid L-arginine by a family of nitric oxide synthases. It plays a role in many physiological functions such as the inhibition of platelet aggregation and regulation of cardiac contractility,[1] and as a neurotransmitter in the central nervous system.[2] However, nitric oxide can have cytotoxic properties at sufficiently high concentrations and it is advantageous to inhibit its formation in several clinical situations such as septic shock, certain chronic inflammatory diseases and epilepsy where overproduction of nitric oxide may lead to neurotoxicity.[3]

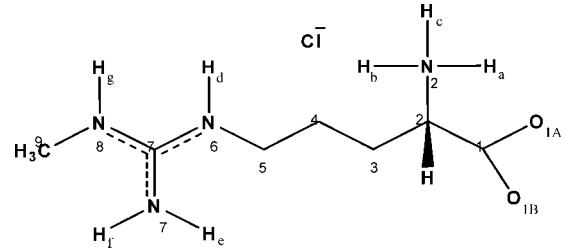

Figure 1. **Molecular structure of Form A of the N^G-monomethyl L-arginine hydrochloride molecule, illustrating the important hydrogen donor atoms that participate in hydrogen bonding in both forms A and D.**

The generation of nitric oxide from L-arginine can be inhibited by several analogues of L-arginine of which the methylated L-arginine analogue, N^G-monomethyl-L-arginine (L-NMMA), shown in Figure 1, was the first to be identified. L-NMMA, found to act as a competitive inhibitor during the production of nitric oxide synthase, has been the subject of several clinical trials.[4−6] There has also been a great deal of recent interest in using L-NMMA as a tool in understanding the relevance of NO in biological processes.[7−10]

* r.b.hammond@leeds.ac.uk.

† Institute of Particle Science and Engineering, School of Process, Environmental and Materials Engineering, University of Leeds.

‡ School of Chemistry, University of Leeds.

§ School of Crystallography, Birkbeck College.

(1) Moncada, S.; Higgs, A. *N. Engl. J. Med.* **1993**, *329*, 2002–2012.
(2) Garthwaite, J. *Trends Neurosci.* **1991**, *14*, 60–67.
(3) Moncada, S.; Higgs, A.; Furchgott, R. *Pharma Rev.* **1997**, *49* (2), 137–142.
(4) Ashina, M.; Lassen, L. H.; Bendtsen, L.; Jensen, R. *J. Lancet* **1999**, *353* (9149), 287–289.
(5) Freeman, B. D.; Danner, R. L.; Banks, S. M.; Natanson, C. *Am. J. Respir. Crit. Care Med.* **2001**, *164* (2), 190–192.
(6) Calles-Escandon, J.; Cipolla, M. *Endocr. Rev.* **2001**, *22* (1), 36–52.
(7) Quezado, Z. M. N.; Karzai, W.; Danner, R. L.; Freeman, B. D.; Yan, L.; Eichacker, P. Q.; Banks, S. M.; Cobb, J. P.; Cunnion, R. E.; Quezado, M. J. N.; Sevransky, J. E.; Natanson, C. *Am. J. Respir. Crit. Care Med.* **1998**, *157* (5), 1397–1405.
(8) Vega, M.; Urrutia, L.; Iñiguez, G.; Gabler, F.; Devoto, L.; Johnson, M. C. *Mol. Hum. Reprod.* **2000**, *6* (8), 681–687.
(9) Valance, P.; Chan, N. *Heart* **2001**, *85*, 342–350.
(10) Alcaraz, M. J.; Guillén, M. I. *Curr. Pharm. Des.* **2002**, *8* (3), 215–231.

Published on Web 08/26/2008
10.1021/op700171b CCC: $40.75

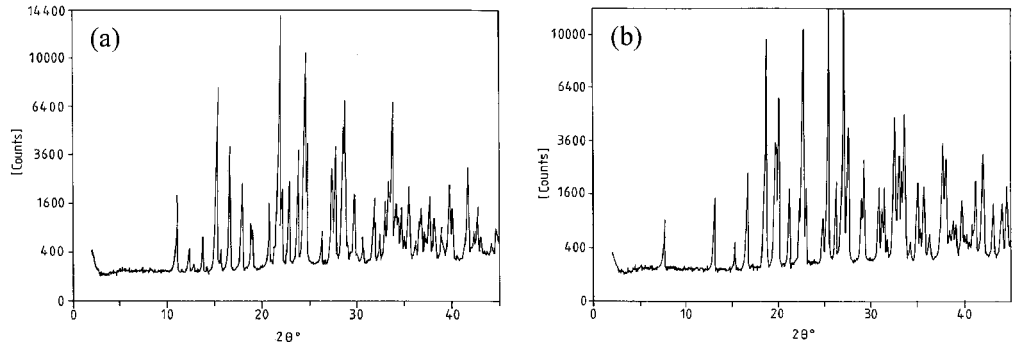

Figure 2. **X-ray powder diffraction patterns of the polymorphic forms of L-NMMA·HCl: (a) Form A and (b) Form D.**

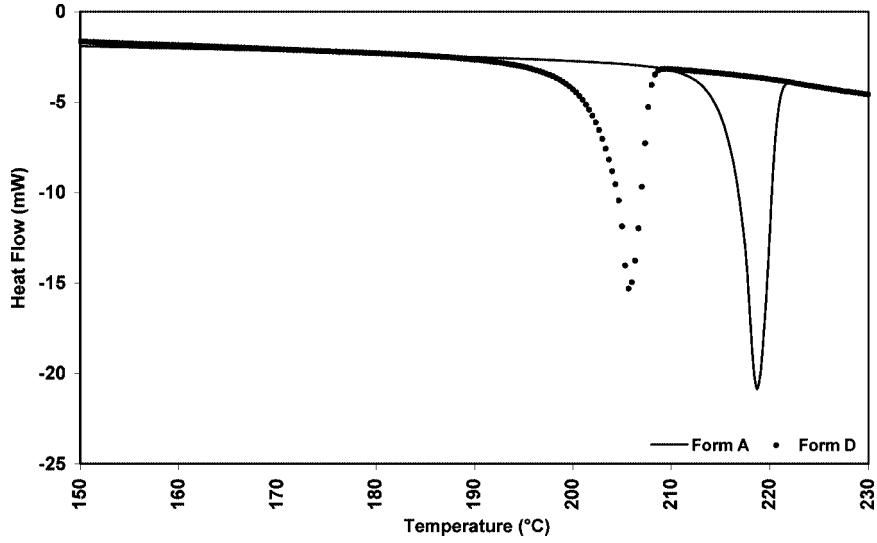

Figure 3. **DSC heat flow curves illustrating the melting behavior of Form A (solid line) and Form D (dotted line) during heating using a heating rate of 5 °C/min.**

N^G-monomethyl-L-arginine hydrochloride, L-NMMA·HCl, a methylated hydrochloride salt, was developed primarily to treat septic shock and two polymorphs (A and D) were identified. Powder X-ray diffraction (PXRD) patterns[11] and differential scanning calorimetry (DSC) heat-flow curves of the two forms are shown in Figures 2 and 3. In this article, forms A and D are compared and contrasted in terms of their molecular conformation, crystalline structure and thermodynamic stability. This pharmaceutical material has provided a particularly indicative case study for investigating aspects of structural and physical chemistry that determine the process engineering required to deliver a given polymorph consistently and robustly.

Materials and Methods

The material from which crystals of both forms were grown was provided by GlaxoSmithKline, formerly Glaxo-Wellcome (Stevenage, U.K.) with purity of >97% as determined using high pressure liquid chromatography HPLC.

Material Synthesis and Solid-form Isolation. L-NMMA·HCl was synthesized on an industrial pilot-plant scale using two main production routes, herein after referred to as routes 1 and 2, with all synthetic preparative work carried out at GlaxoSmithKline.[11]

In the route 1 method, a mixture of L-ornithine hydrochloride, *N*,*S*-dimethylthiouronium iodide and sodium hydroxide was stirred for 5 h before cooling and acidification, using hydrochloric acid, to pH 3. The product was then isolated via ion-exchange chromatography using a Dowex 50W-X8 (H^+) ion-exchange resin and eluted with 0.5 M aqueous ammonia. The product fractions were concentrated, acidified using hydrochloric acid to pH 4 and treated with charcoal before filtration and further concentrating by evaporation at 50 °C under reduced pressure. The residue was crystallized by dissolving it in a mixture of industrial methylated spirit (IMS) and water, heating to boiling point, and subsequently cooling to 0−5 °C. The crystallized L-NMMA·HCl was isolated by filtration and dried at 55 °C under vacuum.

In the route 2 method, a mixture of water, lithium hydroxide, L-ornithine hydrochloride and pyrazole *N*-methylcarboxamidine hydrochloride was stirred at 50 °C for 5 h before being cooled to 10−15 °C and acidified using hydrochloric acid to pH 5. The solution was then crystallized in IMS at 0−20 °C. The crystallized crude L-NMMA·HCl was isolated by filtration and dried at 55 °C under vacuum. As this method does not employ a specific purification step prior to crystallization, this process route is generally referred to as a "crude" method.

An analysis of the 35 available batches, provided by GlaxoSmithKline, with total weight of over 250 kg revealed one batch from route 1 (12.1 kg) to contain exclusively

(11) Private communications from Latham, D.; Blake, P.; Price, C. J.; and Ismay, R. A. GlaxoSmithKline, Stevenage, U.K.

polymorph A, whilst all remaining batches from route 2 were found to contain polymorph D exclusively in 27 batches (204 kg in total), polymorph A in 5 batches (27 kg) and a mixture of A and D in 2 batches (10 kg). On the basis of this distribution of the polymorphs amongst the available batches of material, it can be seen that a definite relationship between synthetic route and the polymorphic form cannot be established at present, given that only a single batch of material from Route 1 has ever been available.

Growth of Single Crystals for Structure Determination. A cursory examination of the molecular structure of L-NMMA·HCl reveals a large number of hydrogen bond donor and acceptor atoms, seven and three respectively, and thus, it is not surprising to find that the compound has high aqueous solubility. Hence, in practical terms, mixed solutions of water and alcohol were found to yield the best environment for crystallization. It should be noted that the high viscosity of the compound in solution, combined with a very wide metastable-zone, leads to very challenging crystallization conditions. Consequently, after considerable experimental endeavor to optimize the conditions, Form A crystals, suitable for single crystal X-ray diffraction, were grown through slow evaporation of a solution of L-NMMA·HCl and 70:30 ethanol:water (vol %). Crystals of Form D were obtained through slow evaporation of a solution of L-NMMA·HCl and 80:20 ethanol:water (vol %). It should be noted that the slight difference in the solvent composition of the solutions used to grow single crystals of forms A and D does not indicate that this is the dominant factor that controls the polymorphic form produced. Mixed solvents with these compositions can yield either polymorph.

Single Crystal X-ray Structure Determination. A single crystal of Form A was mounted on a Nonius CAD4 diffractometer and irradiated with Cu Kα X-rays (λ = 1.54178 Å). Indexing, data collection strategy, data collection control, integration, scaling, space-group determination, structure solution and refinement were achieved using CAD-4 Express-88 software.[12] During the indexing and data collection procedure, the crystal temperature was maintained at room temperature. The position of the Cl atom was determined from the Patterson function, and the organic molecule was located from electron density maps calculated on the basis of phases initially derived from the Cl position. The location of all non-hydrogen atoms was carried out in this way. The tentative structural model was refined using the program SHELXL-97[13] initially with isotropic thermal parameters and subsequently in anisotropic mode. The absorption surface of the crystal was plotted using DIFFABS;[14] the absorption corrected data were used throughout the subsequent refinement. For all hydrogen atoms, apart from those on the CH_3 group, the positions of hydrogen atoms were located on difference electron density maps with subsequent refinement of the atomic fractional coordinates (x,y,z) and isotropic thermal parameter (U_{iso}). For the CH_3 group, hydrogen atoms were inserted into geometrically idealized positions and then oriented by the refinement of their torsion angles into the electron density. The presence of the chloride anion produced anomalous scattering effects with Cu Kα radiation sufficient to assign the absolute configuration of the structure (Flack parameter = 0.00 with esd = 0.02).

A single crystal of Form D was mounted on a Nonius KappaCCD diffractometer (Bruker AXS B.V., Delft, The Netherlands) and irradiated with Mo Kα X-rays (λ = 0.71073 Å). Indexing, data collection strategy, data collection control, integration, scaling, space-group determination, structure solution and refinement were achieved using COLLECT2003 (Bruker AXS B.V.) and its embedded programs DENZO-SMN,[15] maXus,[16] SHELX-97 and SHELXL-97.[13] Intensity data to 99.9% completeness were recorded using φ- and ω- scans of 2.0° and a crystal-to-detector distance of 29.0 mm. During the indexing and data collection procedure, the crystal temperature was maintained at 150 ± 2 K using an Oxford Crystream 600 system. All non-hydrogen atoms were refined anisotropically. All hydrogen atoms could be located in the Fourier difference map and were refined isotropically with no restraints. An absorption correction was not applied. The presence of the chloride anion produced anomalous scattering effects sufficient to assign the absolute configuration of the cation (Flack parameter = 0.00 with esd = 0.05).

Molecular Modeling Approaches. A comparative study of the molecular and solid-state structures of polymorphs A and D was undertaken using the initial specification of the molecular geometry taken from the solved crystal structures. The study employed first a semiempirical molecular orbital approach, using the computer programme MOPAC,[17] and second a molecular mechanics approach using the routines available in the Cerius[2] programme package.[18] In addition, the energy minimized structures were fully visualized with the intermolecular packing configuration analyzed via the graph set method.

The protocol adopted for the MOPAC calculations of molecular-conformation energetics was as follows. A single self-consistent-field calculation (keyword 1SCF) was performed using the AM1 and PM3 methods on the molecular geometries of the cations taken from the single crystal structure determinations for the two polymorphs. The molecular cations were further subjected to geometry optimization in two stages. First, just the hydrogen atoms were relaxed and second, all the atoms were relaxed. Finally, an internal reaction-coordinate calculation was performed to assess the energy barrier to the internal rotation that relates the different conformations observed in the molecular cations of the two polymorphs.

The protocol adopted for the molecular mechanics calculations using Cerius[2] for solid-state packing energetics was as follows. The Dreiding force field[19] was employed, and the Ewald summation method was used for calculation of the electrostatic component of the energy. Care was taken to assign the correct force-field parameters to describe the atoms in the guanidinium moiety. Sets of atomic point charges were

(12) *Enraf-Nonius, CAD-4 Software*; Enraf-Nonius: Delft, Holland, 1998.
(13) Sheldrick, G. M.; *SHELX97 Programme for the refinement of crystal structures*; University of Göttingen: Göttingen, Germany, 1997.
(14) Walker, N.; Stuart, D. *Acta Crystallogr.* **1983**, *A39*, 158–66.
(15) Otwinowski, Z.; Minor, W. *Methods Enzymol.* **1996**, *276*, 307–326.
(16) Mackay, S.; Dong, W.; Edwards, C.; Henderson, A.; Gilmore, C.; Stewart, N.; Shankland, K.; Donald, A. *MaXus Users Manual*; University of Glasgow: Scotland, 1999.
(17) Stewart, J. J. P. *J. Comput.-Aided Mol. Des.* **1990**, *4*, 1–105.
(18) *Cerius*[2] *Molecular Modelling Software for Materials Research* Accelrys Inc.: Princeton, NJ, 2000.
(19) Mayo, S. L.; Olafson, B. D.; Goddard, W. A., III *J. Phys. Chem.* **1990**, *94*, 8897–8909.

Table 1. **Single crystal X-ray experimental and structure refinement details**

crystal data	Form A	Form D
chemical formula	$C_7H_{17}N_4O_2 \cdot Cl$	$C_7H_{17}N_4O_2 \cdot Cl$
M_r	224.70	224.70
cell setting, space group	orthorhombic, $P2_12_12_1$	monoclinic, $P2_1$
a, b, c (Å)	8.541 (2), 9.930 (4), 13.776 (9)	5.4940 (2), 8.3570 (2), 11.885 (4)
β (deg)		102.0500 (10)
V (Å^3)	1156.1 (9)	533.66 (3)
Z	4	2
D_x (Mg m^{-3})	1.297	1.398
radiation type	Cu Kα	Mo Kα
no. of reflections for cell parameters	25	4826
θ range (deg)	16.22−71.90	1.0−27.5
μ (mm^{-1})	2.831	0.34
temperature (K)	293(2)	150 (2)
crystal size (mm^3)	0.3 mm × 0.3 mm × 0.2 mm	0.12 mm × 0.09 mm × 0.04 mm
diffractometer	Nonius CAD4	Nonius KappaCCD area-detector
data collection method	ω/φ scans	φ and ω scans to fill the asymmetric unit
no. of measured, independent, and observed reflections	1488, 1423, 1004	7358, 2075, 1954
R_{int}	0.0227	0.041
refinement on	F	F^2
$R[F^2 > 2\sigma(F^2)]$, $wR(F^2)$, S	0.0392, 0.1016, 1.012	0.028, 0.064, 1.04
no. of relections/parameters	1423/185	2075/195
H-atom treatment	refined independently	refined independently
weighting scheme	calculated $w = 1/[\sigma^2(F_o^2) + (0.0683P)^2 + 0.0000P]$ where $P = (F_o^2 + 2F_c^2)/3$	calculated $w = 1/[\sigma^2(F_o^2) + (0.0086P)^2 + 0.1024P]$ where $P = (F_o^2 + 2F_c^2)/3$
$(\Delta/\sigma)_{max}$	<0.0001	<0.0001
$\Delta\rho_{max}$, $\Delta\rho_{min}$ (e Å^{-3})	0.094, −0.075	0.15, −0.20

calculated using the Gasteiger[20] method. The single crystal structures were subjected to optimization of the total energy in the following way. First, the intermolecular energy terms were evaluated using rigid-body definitions where the molecular cation and chloride anion were defined together as a single rigid body. Second, a two-step process was employed in which, initially, just the positions of the hydrogen atoms and then, in a subsequent step, the positions of all the atoms were allowed to relax in the context of the crystal lattice. These steps were performed without allowing the cell parameters describing the structure to relax, and following this, the structures were then further optimized by allowing the cell parameters to relax to compare the changes effected as a result of this.

Molecular visualization facilities in the programme suite, Cerius[2], were employed to examine and compare the molecular packing and intermolecular hydrogen-bonding motifs in the polymorphs prior to, and after, the various energy minimization steps and to measure structural parameters such as bond lengths, bond angles, and torsion angles. The intermolecular hydrogen bonding was analyzed using the graph-set method.[21,22] This involved the identification of repetitive motifs among the hydrogen bonds present and the assignment of a graph type to characterize a particular motif as infinite (C), cyclic (R), intramolecular (S), or dimeric (D) along with the inclusion of number of proton acceptors and donors and the size of the motif with the graph type as superscripts, subscripts, and in parenthesis, respectively.

(20) Gasteiger, J.; Marsili, M. *Tetrahedron* **1980**, *36*, 3219–3228.
(21) Etter, M. C.; MacDonald, J. C.; Bernstein, J. *Acta Crystallogr.* **1990**, *B46*, 256–262.
(22) Bernstein, J.; Davis, R. E.; Shimoni, L.; Chang, N. *Angew. Chem., Int. Ed. Engl.* **1995**, *34*, 1555–1573.
(23) Burger, A.; Ramberger, R. *Mikrochim. Acta [Wien]* **1979**, 259–271.
(24) Ladd, M. F. C.; Palmer, R. A. *Structure Determination by X-ray Crystallography*, 4th ed; Kluwer/Plenum: New York, 2003.

Examination of Polymorphic Stability. Differential scanning calorimetry (DSC) measurements were carried out to investigate the thermal behavior of the two polymorphs using a Mettler Toledo DSC 820 with a TS0801R0 automatic sampler. Small weighed quantities of each form were sealed in 40 μL aluminium sample holders and heated over a temperature range of 25−300 °C using heating rates of 2, 5, 10, and 20 °C/min, under a nitrogen purge. The effects of heating rates on the DSC data were corrected using a τ evaluation.

The relative stability of the polymorphs was investigated, at 50 °C, by monitoring whether any solvent-mediated transformation between the forms could be identified. Hence, mixtures of equal masses of forms A and D were stirred for periods of over 24 h at 50 °C in mixed solvents (saturated with the solute) consisting of water and an alcohol (methanol or ethanol), with compositions of 90:10 and 80:20 (vol %). The resulting solids were separated by filtration, allowed to dry, and then tested for their polymorphic composition using powder X-ray diffraction. A Siemens D500 powder X-ray diffractometer with Cu Kα radiation and a secondary curved graphite monochromator was employed to obtain the diffraction profiles of the powders in flat plate Bragg−Brentano mode within a range of $2\theta = 3-40°$ with a step size of 0.02° and a dwell time of 1 s/step.

Results and Discussion

Crystal Structure and Molecular Conformation Determined for Forms A and D. The full crystal structural data for forms A and D have been deposited in the Cambridge Crystallographic Database, reference codes CCDC279936 and CCDC290601, respectively.

Given that the molecule N^G-methyl-L-arginine is an optically pure form (a derivative of an L-amino acid), it can crystallize in space groups which have only rotational axes of symmetry.

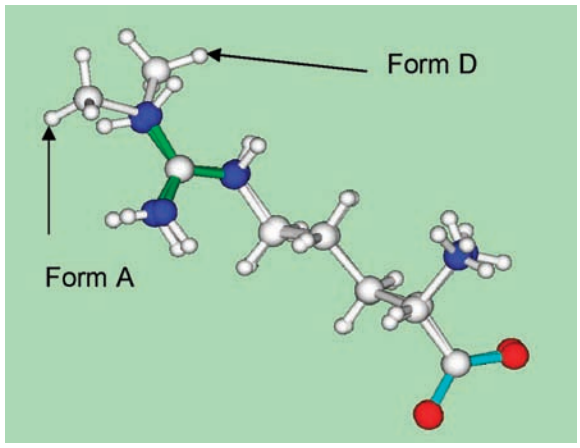

Figure 4. **Overlay of molecular structures taken from the solved crystal structures of Forms A and D, revealing that the *N*-methyl group has a *cis* configuration in Form D but a *trans* configuration in Form A.**

This is because centres of symmetry, mirror planes and glide planes would necessarily involve both L- and D-amino acid forms. As a consequence the enantiomerically resolved crystals can only exist in 65 space groups of the possible 230.[24] The enantiomorphic class for the orthorhombic system is 222, the space group of polymorph A, $P2_12_12_1$, belongs to this class. Similarly for the monoclinic system it is the polar class 2 which includes the space group of polymorph D, $P2_1$. Table 1 summarizes the structural refinement data for the two polymorphic forms showing that the unit cell volume of Form A is more than double that of Form D, although structure determinations of both forms were carried out at different temperatures. In this, Form A was found to contain four L-NMMA·HCl formula units per unit cell compared to two for Form D. Calculation of the densities for the two forms, based on the crystallographic structures, reveals A and D to be 1.3 and 1.4 (Mg m^{-3}), respectively, and in agreement with the proposed structural stabilities, i.e. the more densely packed form is found to be consistent with the greater structural stability. In both polymorphs the asymmetric unit was found to consist of a single molecule of N^G-monomethyl-L-arginine hydrochloride. Figure 1 shows the molecular structure and the atom numbering for Form A.

The molecular conformation of the cation in forms A and D was found to be similar and is depicted in Figure 4 where cations from the two forms are overlaid. The main difference in the conformation is in the relative orientation of the *N*-methyl group. In the guadinium moiety there is restricted rotation about the three covalent bonds to the carbon atom. Consequently, it is convenient to identify two geometric isomers; the Z isomer is manifested in Form D and the E isomer in Form A, and for the purposes of discussion these are referred to as "*cis*" in Form D and "*trans*" in Form A. Molecular packing diagrams of both forms are shown in Figure 5 with the hydrogen bonds represented by black dashed lines. In the case of polymorph D, the polar direction is clearly manifested in the molecular packing of this form as Figure 5b.

Description of Crystal Packing and Hydrogen Bonding of Forms. The unit cell of Form A contains four asymmetric units. The units are organized in pairs that interact through the formation of chains along the crystallographic *a*-axis in which a hydrogen atom of the α-amino moiety forms a hydrogen bond with an oxygen atom from the other molecule. The chains so described stack in the direction of the crystallographic *b*-axis. Observing the packing in projection along the *a*-axis, as shown in Figure 5b, adjacent stacks are displaced by a half-lattice-spacing along the *b*-axis. The stacks interleave so that the carboxylic acid groups of a pair of molecules in one stack form two hydrogen bonds, separately, with the guadinium moiety of a molecule in one of the two adjacent stacks. Molecules of adjacent stacks are also linked through chains of hydrogen bonds aligned with the *b*-axis. The chains involve a hydrogen atom of the α-amino moiety of a molecule residing alternately in the first and second stack interacting with the same chloride ion.

The asymmetric unit contains seven hydrogen atoms that can be donated to form hydrogen bonds (four in the guadinium moiety and three in the α-amino group) and three acceptor atoms (two carboxylate oxygens, and one chloride ion). The network of hydrogen bonds interconnects the asymmetric units so that the carboxylate oxygen atoms accept the hydrogen atoms H_d and H_g from the secondary amine groups, one of the two hydrogen atoms, H_e, bonded to atom N_7 and one of the three hydrogen atoms, H_a, of the α-amino group. Both secondary amine groups on one cation hydrogen bond to the same oxygen atom of a cation in an adjoining stack. The other hydrogen atom in the primary amine group of the guadinium moiety, H_f, forms a hydrogen bond with a chloride ion. In addition the chloride ions accept hydrogen bonds from atoms, H_b, and H_c. A specific chloride ion interacts with one hydrogen atom on three different molecular cations.

The hydrogen-bonding interactions observed in Form A were characterized using graph set analysis. It is customary to use letters taken in alphabetical order to identify the unique hydrogen bonds. In this instance there are seven unique hydrogen bonds; three, a, b and c, involve the hydrogen atoms bonded to the α-amino group nitrogen (N_2); one, d, involves the hydrogen atom bonded to nitrogen N_6; two, e and f, involve the hydrogen atoms bonded to N_7; and one, g, involves the hydrogen bonded to N_8. The first-order graph set for Form A can be divided into two parts. First, four of the unique hydrogen bonds a, d, e, and g arise from hydrogen bonding between the molecular cations only; this subset is $N_1 = C(5)C(8)C(10)C(10)$. Second, the other three hydrogen bonds involve the chloride ion and accordingly have the designation D in the first-order graph set. Examination of the hydrogen bonding surrounding the chloride ions reveals that chain motifs are chiefly formed and belong to second- or higher-order graph sets. However, motifs surrounding a fully hydrogen-bonded chloride ion, accepting hydrogen bonds from three donor atoms, only become apparent at the fourth order, where with additional acceptor atoms from the cation moieties, two interconnecting cyclic or ring motifs, $R_4^2(8)$, are observed. The first section of Table 2 summarizes the results of the graph set analysis of Form A.

The crystal structure for Form D contains two asymmetric units in the unit cell related by the 2_1 screw axis. The carboxylate oxygen atoms accept two hydrogen bonds each from four donor atoms belonging to four different molecular cations. The

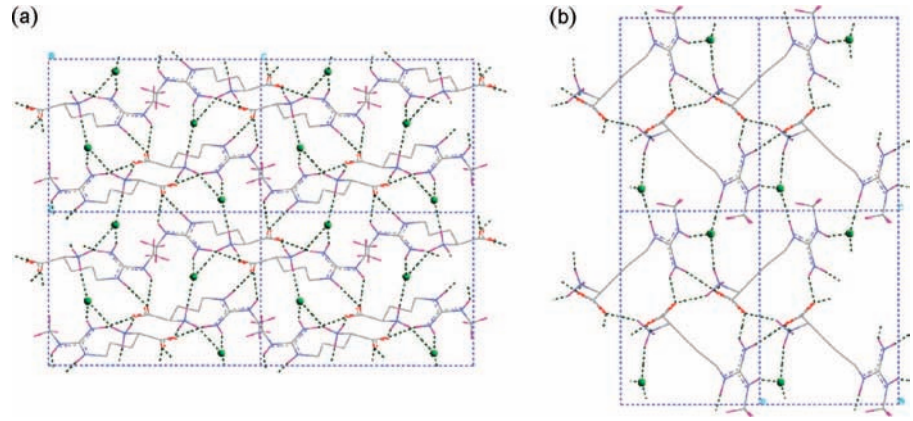

Figure 5. **Molecular packing diagrams for polymorphs (a) A and (b) D both shown along the crystallographic axes, *a*. Please note that the hydrogen atoms bonded to carbon atoms have been omitted for clarity.**

Table 2. **Hydrogen-bonding geometry in polymorphs A and D described using graph set analysis illustrating the different motifs located at first and second orders[a]**

Form A	a	b	c	d	e	f	g
a	C 5[a]						
b	D_3^3 10[a]	C 2[a]					
c	D_3^3 10[a]	D_2^1 4[a]	D 2[a]				
d	D_2^2 11[a]	D_3^3 15[a]	D_3^3 10[a]	D 8[a]			
e	D_2^1 10[a] and D_2^2 15[a]	D_3^3 17[a]	D_3^3 17[a]	D_2^2 8[a]	D 10[a]		
f	D_3^3 10[a]	D_2^1 11[a]	D_2^1 11[a]	D_3^3 17[a]	D_3^3 17[a]	D 2[a]	
g	D_2^2 13[a]	D_3^3 17[a]	D_3^3 17[a]	D_3^3 10[a]	D_2^2 8[a]	D_3^3 17[a]	D 10[a]

Form D	a	b	c	d	e	f	g
a	C 2[a]						
b	D_3^3 10[a]	C 5[a]					
c	D_3^3 10[a]	D_2^2 6[a]	D 5[a]				
d	D_2^1 9[a]	D_3^3 18[a]	D_3^3 18[a]	D 2[a]			
e	D_3^3 17[a]	D_2^2 13[a]	D_2^1 11[a]	D_3^3 15[a]	D 10[a]		
f	D_3^3 17[a]	D_2^1 11[a] and R_2^2 15[a]	D_2^2 13[a]	D_3^3 15[a]	D_2^2 6[a]	D 17[a]	
g	D_2^1 11[a]	D_3^3 22[a]	D_3^3 22[a]	D_2^1 6[a]	D_3^3 17[a]	D_3^3 17[a]	D 2[a]

[a] Here, a, b, and c refer to the hydrogen atoms from the α-amino group, d and g from the two secondary amine groups, and e and f from the primary amine group.

carboxylate oxygen atom O_{1A} accepts intermolecular hydrogen bonds from atoms H_f and H_b, and oxygen O_{1B} accepts hydrogen bonds from donor atoms H_c and H_e. The hydrogen bonds between the acceptor atom O_{1A} and atoms H_b and H_f from the α-amino and primary amine groups, respectively, were found to propagate along the polar *b*-axis as a result of the intermolecular bond $N_2-H_b\cdots O_{1A}$ linking molecular cations in adjoining planes. This is shown in Figure 5b where the polar axis can be clearly seen. The chloride ion was found to accept three hydrogen bonds from atoms H_d, H_a, and H_g which originate from three different molecular cations. Two of these molecular cations are symmetrically related to one another by translation with the third cation related to the others by translational and rotational symmetry.

The first-order graph for form D is designated $N_1 = C(5)C(10)C(5)C(10)$ resulting from chain motifs formed by hydrogen bonds b, c, e, and f between the molecular cation moieties only. The chain motifs $C(10)$ describe the intermolecular bonding involving donor atoms from primary amine groups, e and f, and the shorter chain motifs $C(5)$ involve intermolecular bonds from two donor atoms of the α-amino group. The hydrogen bond motifs surrounding the chloride ion only become apparent in the higher-order graph sets. The second-order graph set describing the intermolecular bonding surrounding the chloride ions consists of chain motifs that connect molecular ions in adjacent unit cells. This was seen to create a network of intermolecular hydrogen bonds that can be described as large spiraling chains, $C_4^2(15)$, a fourth-order graph set. The graph set analysis for Form D is summarized in the second part of Table 2.

Table 3. **Comparison of the involvement of different donor groups with acceptor atoms (1) O_{1A}, (2) O_{1B}, and (3) Cl in forms A and D[a]**

donor group	Form A	Form D
a	2	2
b	3	1
c	3	3
d	1	3
e	2	2
f	3	1
g	1	3

[a] Here, a, b, and c refer to the hydrogen atoms from the α-amino group, d and g from the two secondary amine groups, and e and f from the primary amine group.

Comparison of the Structures of Forms A and D. The variation in hydrogen bonding, as manifested in the different packing arrangements of the forms, results from differences in the conformation of the molecular cation. The *cis* and *trans* configurations lead to the pairing of different combinations of

Table 4. **Form A: hydrogen-bonding geometry resulting from the optimization of the whole unit cell, minimized with rigid-body constraints[a]**

D	H	A	D−H	H−A	DHA[b]
N_2	H_a	O_{1B}	2.99	2.05	154.7
N_2	H_b	Cl	3.22	2.27	155.6
N_2	H_c	Cl	3.13	2.12	174.9
N_6	H_d	O_{1A}	2.73	1.84	158.4
N_7	H_e	O_{1B}	2.87	1.95	158.7
N_7	H_f	Cl	3.36	2.44	157.9
N_8	H_g	O_{1A}	3.18	2.38	138.6

[a] The D−H and H−A distances are in Å and DHA angles in deg. [b] DHA: donor, participating hydrogen and acceptor atoms used to denote hydrogen bonding components.

Table 5. **Form D: hydrogen bonding geometry resulting from the optimization of the whole unit cell minimized with rigid body constraints[a]**

D	H	A	D−H	H−A	DHA[b]
N_2	H_a	Cl	3.09	2.20	145.7
N_2	H_b	O_{1A}	2.87	1.95	150.5
N_2	H_c	O_{1B}	2.85	1.98	143.2
N_6	H_d	Cl	3.10	2.20	155.1
N_7	H_e	O_{1B}	2.89	2.11	148.3
N_7	H_f	O_{1A}	2.98	2.11	148.3
N_8	H_g	Cl	3.13	2.25	152.3

[a] The D−H and H−A distances are in Å and DHA angles in deg. [b] DHA: donor, participating hydrogen and acceptor atoms used to denote hydrogen bonding components.

donor and acceptor atoms apart from the intermolecular bond $N_7-H_e\cdots O_{1B}$ which is common to both polymorphs. The *trans* configuration of Form A has the donor atoms H_d and H_g oriented in the same direction, and these are accepted by the same atom, O_{1A}. In contrast, the *cis* configuration in Form D has atoms H_d and H_g oriented in different directions, and these are accepted by two different chloride ions. As a result, each ionic pair in Form A requires donor and acceptor atoms from six different cations and two chloride ions to realize its full hydrogen-bonding potential, whereas Form D requires seven cations and two chloride ions to be fully hydrogen bonded. Differences in the pairing of hydrogen bond donor and acceptor atoms for the two forms are summarized in Table 3. Tables 4 and 5 list the hydrogen bond lengths and angles measured in the crystal structures of the two forms observed between the seven available donor atoms and three acceptor atoms.

Despite the differences observed in hydrogen-bonding interactions of the two forms, certain common features can be observed. The first-order graph sets, for example, consist solely of chain motifs in both forms, involving intermolecular bonding between the cation moieties only. Although the four chain motifs in the first-order graphs sets for both forms describe the intermolecular bonding between the carboxylate oxygen acceptor atoms and different proton donor atoms, three of the four chain motifs, $C(5)$ and $C(10)$, are identical in both forms. Certain motifs in the second-order graph sets are also common to both forms. For example the chain motifs $C_2^2(13)$ associated with intermolecular bonding linking the carboxylate oxygen atoms, $C_2^1(11)$ involving the bonding environment surrounding the chloride ion and the spiraling chain motif $C_2^2(15)$ connecting one donor atom from the α-amino and primary amine groups to the carboxylate oxygen atoms are identical in both forms.

In addition, another common motif involves hydrogen bonding between three molecular cations and a chloride anion; the participating functional groups, however, are found to be quite different between the two forms. The chloride ion in Form A accepts hydrogen bonds from N_2-H_b, N_2-H_c, and N_6-H_d groups, whilst in Form D hydrogen bonds are accepted from N_6-H_d, N_2-H_a, and N_8-H_g groups. Figure 7 illustrates the respective packing motifs of the three cations associated with a common chloride ion for both forms A and D. The ring motif $R_4^2(8)$ describing the intermolecular bonding involving the chloride ions is also common between the two forms along with the chain motifs that link the ring motifs, albeit the notation of chain motifs is $C_2^1(4)$ in Form A and $C_2^1(11)$ in Form D.

However, more graph set patterns were observable in Form D than Form A. This is clearly a manifestation of the different space group symmetry operating in the two polymorphs and its impact on the relative orientation of neighbouring molecules in the first coordination sphere about an asymmetric unit. In one sense, Form A manifests a more efficient arrangement in fully satisfying the hydrogen-bonding capacity of the asymmetric unit by hydrogen bonding to just six rather than seven neighbouring cations, but nevertheless, this results in a less close-packed arrangement as reflected in the lower density of Form A.

A further interesting feature of these two structures is reflected in the local molecular environment around the chloride counterion. Here, the multiplicity of the potential donors can be differentiated in terms of the position of these functional groups with respect to the different ends of the molecules towards the chloride ion. Considering these end positions, i.e. the close proximities of the α-amino group to the carboxylic end of the molecule and the primary and the two secondary amine groups to the *N*-methyl end, there can, in principle, be four combinations of molecular orientations surrounding the chloride ion: MMM, CCC, CCM, and CMM, where M and C denote the *N*-methyl and carboxylic acid ends. Two of these combinations can be observed in Figure 7, where Form A adopts the CCM orientation and Form D adopts the CMM orientation. Tentatively, one could suggest that the remaining packing motifs (MMM and CCC) might be associated with further polymorphic forms. Interestingly, also, the two different conformers are not seen together in the same structure, i.e. via mirror symmetry, and this too might offer the potential for further polymorphic forms. The richness of the bonding possibilities, in terms of packing density, would clearly have value for further study.

Structural Stability and Mechanism for Phase Interconversion. SCF calculations using MOPAC were carried out to assess the energy barrier to the internal rotation of the nitrogen atom, N_8, connected to the *N*-methyl functional group and the central carbon atom of the guanidine group, as the difference between the two forms is in the orientation of the *N*-methyl group. These calculations were conducted as a function of the degree of rotation imposed upon the nitrogen atom, N_8, and the *N*-methyl group with the enthalpy of formation calculated for each structure. The results of the calculations are shown in Figure 6. The energy barrier for the rotation of the terminal

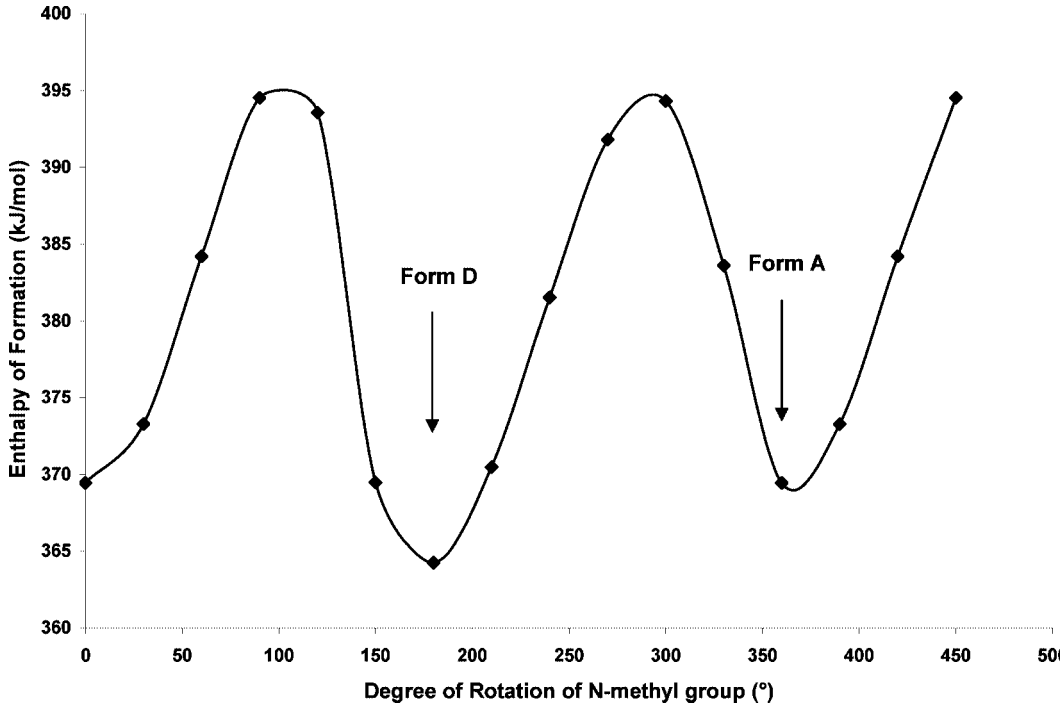

Figure 6. **Calculated molecular enthalpy of formation as a function of degree of internal rotation of the terminal *N*-methyl group and illustrating the relative molecular energetic stabilities for forms A and D at their degrees of rotations. The degree of rotation and the corresponding enthalpic values have been repeated beyond 360° for better visual clarity of the relative stabilities associated with polymorphs A and D on the plot.**

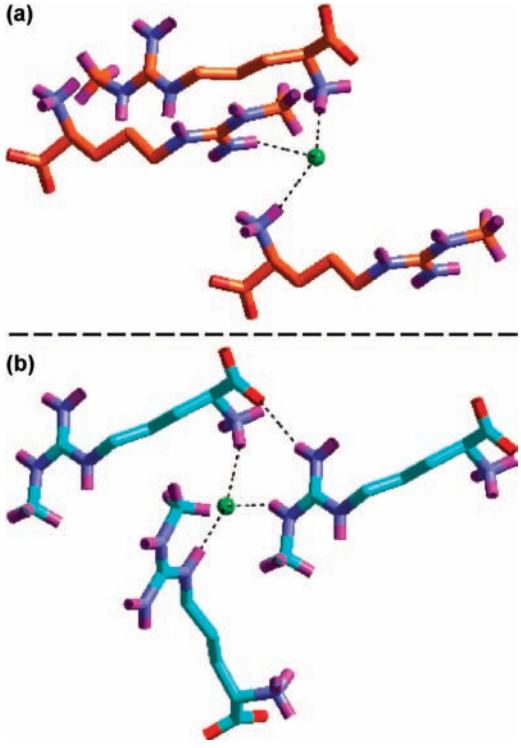

Figure 7. **Local molecular environment round the Cl counterion of Form A (a, top) and Form D (b, bottom) showing the participation of different functional groups in hydrogen bonding with a central chlorine ion. The Cl ion in Form A accepts hydrogen bonds from N_2-H_b, N_2-H_c, and N_6-H_d groups, whereas the Cl ion in Form D accepts from N_6-H_d, N_2-H_a, and N_8-H_g groups. The hydrogen atoms belonging to the alkyl chain carbon atoms have been omitted for better visual clarity.**

Table 6. **Calculated lattice energies, in kcal/mol, of Forms A and D before and after optimization of structures with fixed cell constants**

	lattice energies for Form A (kcal/mol)		lattice energies for Form D (kcal/mol)	
	before	after	before	after
van der Waals	−4.60	−6.31	−8.76	−7.16
electrostatic	−110.65	−110.18	−115.12	−117.78
hydrogen bonds	−12.18	−12.32	−9.08	−9.79
total (kcal/mol)	−127.44	−128.81	−132.96	−134.73

Table 7. **Calculated lattice energies, in kcal/mol, of Forms A and D before and after optimization of structures with cell constants allowed to vary following prior optimization of structures with rigid body constraints**

	lattice energies for Form A (kcal/mol)		lattice energies for Form D (kcal/mol)	
	before	after	before	after
van der Waals	−6.31	−3.82	−7.16	−7.42
electrostatic	−110.18	−113.70	−117.78	−117.67
hydrogen bonds	−12.32	−13.43	−9.79	−9.78
total (kcal/mol)	−128.81	−130.95	−134.73	−134.87

Table 8. **DSC data for forms A and D showing their melting points, enthalpy of fusion, ΔH_f, and entropy of fusion, ΔS_f, measured using a heating rate of 10°C/min together with the estimated average deviation**

	Form A	Form D	average deviation
melting point (°C)	215.7	203.7	0.33
ΔH_f (kJ/mol)	34.9	35.6	3.21
ΔS_f (J/mol·K)	71.3	74.4	2.88

N-methyl group (in an isolated molecule) at room temperature was found to be approximately 25 kJ/mol. An energy barrier of this magnitude indicates that the conformations can interconvert

at room temperature, and in solution, the molecular cation is probably quite labile with respect to changing its conformation.

The calculated lattice energies are shown in Tables 6 and 7 for the two forms. Comparison of the total energies shows that Form D has a lower intermolecular energy than Form A when the crystal structures are optimized whilst maintaining the cell parameters constant and also when the cell parameters are allowed to relax. The rms change in the atomic distances as a result of allowing the cell parameters to change during the final optimization stage is 1.85 and 2.78% for forms A and D, respectively.

DSC results, shown in Figure 3 and Table 8, are consistent with a monotropic relationship between the two forms with Form A melting at a much higher temperature than Form D and a rather similar enthalpy of fusion, ΔH_f. The higher melting point of Form A suggests its greater stability with respect to Form D, and a closer examination of the enthalpy and entropy of fusion might indicate an enantiotropic relation between the two forms.[23] The DSC data though does not support an enantiotropic relation between the two forms due to the lack of any phase transformation prior to melting.

Powder XRD analysis of dried crystals resulting from solution stability studies showed full transformation to Form D, clearly indicating that Form D is more stable than Form A.

The exact mechanism for polymorphic transformation between the two forms remains uncertain at this time. Clearly, such a transition would be expected to involve a significant and potentially restricted conformational rotation around the *N*-methyl group between the two polymorphic structures. In addition, whilst the respective space groups have a clearly defined group/subgroup relationship, $P2_1$ being a subgroup of $P2_12_12_1$, the DSC data clearly shows no evidence of any associated solid-state transformation that would be expected for an enatiotropic phase transformation. However, the energy barrier associated with the conformational change that would be needed for such a transformation and the concomitant structural reorganization of the α-amino and the two primary amine groups between the two polymorphic forms might be too high for such a transformation. Thus, at this stage, the phase transformation from Form A to Form D would most likely be associated with a solution-mediated, monotropic mechanism associated with the initial dissolution of Form A and the subsequent nucleation and growth of Form D. Further studies are currently in hand to resolve and define this issue and will be reported in a subsequent paper.

Conclusions

The crystal structures of two polymorphs of L-NMMA·HCl were determined from analysis of single crystals and molecular modeling, thermal analysis and solution stability studies were performed to begin to understand how the form manifested via solution crystallization is related to the crystallization environment and to evaluate the relative thermodynamic stability of the forms. Crystallographic analysis of the two known polymorphic forms revealed Form A to be orthorhombic, in a tetramolecular unit cell with space group $P2_12_12_1$ and Form D to be monoclinic, in a bimolecular unit cell with a polar space group $P2_1$. Comparison of conformational differences between the two molecular cations shows a difference in the orientation of the *N*-methyl group, which is *cis* in Form D and *trans* in Form A. Examination of the polymorphic structures reveal the molecules to be linked by a number of hydrogen bonds associated with seven donor and three acceptor atoms which fully participate in intermolecular bonding in both forms. Graph set analysis of the hydrogen bond patterns reveals the hydrogen bond network to consist mainly of chain and ring motifs in both forms with first-order graph sets consisting solely of chain motifs involving intermolecular bonding between the molecular cation moieties only. Intermolecular bonds involving the chloride counterion only become apparent at higher-order graph sets and consist of characteristic chain motifs with the chloride counterions accepting hydrogen bonds from functional groups belonging to three different molecular cation moieties, namely N_2-H_b, N_2-H_c, and N_6-H_d groups in Form A and N_6-H_d, N_2-H_a, and N_8-H_g groups in Form D. Two of the three donor groups in Form A lie towards the carboxylic end of the cation moieties and one towards the *N*-methyl end, whereas in Form D, two of the three donor groups lie towards the *N*-methyl end and one towards the carboxylic end. Different combinations of donor−acceptor group participation, reflected in the molecular cation positions with respect to the chloride counterion, can result in other possible polymorphs. Thermal analysis of the two forms using DSC is mostly consistent with a monotropic relationship between the two forms, albeit the relative melting points perhaps suggest a more complex behaviour. Despite the higher melting point of Form A, solution stability studies, supported by lattice energy calculations, are consistent with Form D being the more stable polymorphic form at room temperature. Hence, the phase interconversion from Form A to D is likely to be associated with a monotropic and solution-mediated mechanism involving the dissolution of Form A and the subsequent growth and nucleation of Form D.

Acknowledgment

This work has been carried out as part of Chemicals Behaving Badly Phase 2, a collaborative project funded by the UK EPSRC together with support from an industrial consortium including ANSYS Europe Ltd, AstraZeneca, Bede Scientific Instruments Ltd., BNFL, Clairet Scientific Ltd., GlaxoSmith-Kline, HEL Ltd., Malvern Instruments, Pfizer and Syngenta. The academic partners are Leeds, Heriot Watt and Newcastle Universities. We gratefully acknowledge all these sponsors and all members of this academic/industrial team and the industrial coordinator L. J. Ford. We gratefully acknowledge GlaxoSmith-Kline for the provision of this material for careful academic study, and we thank in particular D. Latham, P. Lake, C. J. Price, and R. A. Ismay for many helpful discussions. This work forms the Ph.D. study of one of us (S.D.).[25] R.A.P. thanks Dr. M. F. C. Ladd for useful discussions.

Received for review July 31, 2007.

OP700171B

(25) Dharmayat, S Polymorphism in Pharmaceutical Solids: Crystal Nucleation and Growth, Ph.D. Thesis, University of Leeds, 2008 to be submitted.